Critical behavior and dimension crossover of pion superfluidity

Ziyue Wang and Pengfei Zhuang

Physics Department, Tsinghua University and Collaborative Innovation Center of Quantum Matter, Beijing 100084, China

(Received 25 April 2016; published 29 September 2016)

We investigate the critical behavior of pion superfluidity in the framework of the functional renormalization group (FRG). By solving the flow equations in the SU(2) linear sigma model at finite temperature and isospin density, and making comparison with the fixed point analysis of a general $O(N)$ system with continuous dimension, we find that the pion superfluidity is a second order phase transition subject to an $O(2)$ universality class with a dimension crossover from $d_c = 4$ to $d_c = 3$. This phenomenon provides a concrete example of dimension reduction in thermal field theory. The large-N expansion gives a temperature independent critical exponent β and agrees with the FRG result only at zero temperature.

DOI: 10.1103/PhysRevD.94.056012

I. INTRODUCTION

The study of quantum chromodynamics (QCD) phase transitions at finite temperature and density provides a deep insight into the strong interacting matters created in high energy nuclear collisions and compact stars. The QCD symmetry breaking and restoration patterns lead to a very rich phase structure. The extension of the phase diagram from finite temperature and baryon density to finite isospin density is motivated by the investigation of isospin imbalance in the interior of neutron stars [1,2]. The thermodynamic equilibrium systems with finite isospin chemical potential have been widely investigated through lattice simulations [3–7], random matrix theory [8,9], and effective models like the Nambu–Jona-lasinio (NJL) model [10], quark-meson model [11], and linear sigma model [12,13]. It is found that the spontaneous breaking and restoration of the symmetry between charged pions $\pi_\pm$ are connected by a second order phase transition at both zero and finite temperature.

As a nonperturbative method, the functional renormalization group (FRG) [14,15] is applied to Yang-Mills theory [16] and QCD [17]. By solving the flow equations which connect physics at different momentum scales, the FRG shows a great power in describing the critical behavior of the phase transitions which is controlled by quantum and thermodynamic fluctuations. In the framework of FRG, thermal and quantum fluctuations from ultraviolet to infrared limits are encoded through coarse graining and scale transformation, giving reliable predictions on the properties of both continuous and first order phase transitions [14]. Critical exponents and universality class play an extremely important role in the study of QCD phase transitions. Different systems with the same symmetry and dimension should share identical critical exponents and belong to the same universality class, indicating that the collective properties near a continuous phase transition are independent of the dynamical details of the system.

The macroscopic behavior of a thermal equilibrium system is controlled by the low momentum modes and thermodynamical parameters such as temperature and chemical potential. For a system coupled to an external heat bath, the change in the degrees of freedom may lead to a change in the intrinsic symmetry. For instance, the elemental constituents of a QCD system undergo a change from hadrons at low temperature to quarks and gluons at high temperature; this change leads to the deconfinement phase transition. Such thermal effects also lead to a change in the space-time dimension when analyzing the universality class. In thermal field theory, a compactification is performed in the time direction with a periodic or anti-periodic boundary condition. This procedure generates equidistant Kaluza-Klein modes, namely the Matsubara frequencies in thermal field theory. The dimension reduction goes along with the compactification. When the size of a system goes from infinity to 0 along a fixed direction, the fields lose their original dependence on the dimension corresponding to this direction, and this specific dimension is continuously reduced; see the initial research [18] and recent progress [19]. For a system defined in a space-time dimension d, the change in the thermodynamics of the system is equivalent to the change in the dimension from d to $d-1$ [20,21].

Dimension is crucial for the critical behavior of a continuous phase transition, since it is an essential element in the classification of universality classes. The Ginzburg criterion gives the idea of an upper critical dimension [22]. For a theory with dimension greater than 4, the mean field approach is already good enough to describe the critical phenomena. However, when the dimension is less than 4, fluctuations need to be taken into account. In fact, the exact solution to the Gaussian model with spatial dimension 4 gives indeed the same result as the mean field method, despite the difference in understanding the underlying physics. This motivates the expansion in $4-\epsilon$ [23,24], under the assumption that the critical exponents and physical parameters are continuous with the change in dimension. In the framework of FRG, the scale invariance and self-similarity near the critical point are described by the scale invariant fixed point of the flow equations. The critical surface and properties of the flow around the nontrivial fixed point provide a far-reaching description concerning critical exponents and universality class.

Considering the fact that the baryon density suppresses the pion superfluidity, we investigate in this paper the critical behavior of the strongest pion superfluidity in the limit of vanishing baryon density. In this limit we can take the linear sigma model with only mesons. We organize the paper as follows. The large-N and FRG approaches to the SU(2) linear sigma model are separately discussed in Secs. II and III, the numerical solutions, especially the critical exponents of the pion superfluidity, are shown in Sec. IV, and the comparison with a $O(N)$ model in continuous dimension is given in Sec. V. We summarize in Sec. VI.

II. LARGE-N APPROACH TO PION SUPERFLUIDITY

As an effective low-energy model, the linear sigma model exhibits many of the global symmetries of QCD at meson level and is widely used to demonstrate the spontaneous chiral symmetry breaking in vacuum and its restoration at finite temperature [25–28]. At finite isospin chemical potential μ_I, the SU(2) linear sigma model is defined through the Lagrangian density

$$\mathcal{L} = \frac{1}{2}\partial_\mu\phi\partial^\mu\phi + i\mu_I(\pi_1\partial_t\pi_2 - \pi_2\partial_t\pi_1) + U(\phi),$$
$$U(\phi) = \frac{m^2}{2}\phi^2 + \frac{\lambda}{4}\phi^4 - \frac{\mu_I^2}{2}(\pi_1^2+\pi_2^2) - c\sigma, \tag{1}$$

where $\phi = (\sigma, \boldsymbol{\pi})$ is defined as a four-component field constructed by the isoscalar σ and isovector $\boldsymbol{\pi} = (\pi_1, \pi_2, \pi_3)$. In vacuum at $\mu_I = 0$, the $O(4)$ symmetry in chiral limit is explicitly broken to a rotational symmetry $O(3)$ among the three pions in real case with $c \neq 0$. Turning on the isospin chemical potential splits the three pions, and the $O(3)$ symmetry is explicitly broken to $O(2)$ symmetry. When μ_I exceeds the pion mass m_π in vacuum, the symmetry is further spontaneously broken from $O(2)$ to $Z(2)$ and the system enters the pion superfluidity phase.

The spontaneous chiral symmetry breaking and isospin symmetry breaking are described respectively by the chiral condensate $\langle\sigma\rangle$ and charged pion condensate $\langle\pi_+\rangle = \langle\pi_-\rangle$. Considering the relations $\pi_\pm = (\pi_1 \pm i\pi_2)/\sqrt{2}$, one can take alternatively the condensate $\langle\pi_1\rangle$ as the order parameter of pion superfluidity. Separating the quantum fluctuations from the classical mean fields by making a shift $\phi = (\sigma,\pi_1,\pi_2,\pi_3) \to \langle\phi\rangle + \phi = (\langle\sigma\rangle,\langle\pi_1\rangle,0,0) + (\sigma,\pi_1,\pi_2,\pi_3)$, the Lagrangian density becomes

$$\mathcal{L} = \mathcal{L}_{mf} + \mathcal{L}_{\rm int},$$
$$\mathcal{L}_{mf} = \frac{1}{2}\partial_\mu\phi\partial^\mu\phi + i\mu_I(\pi_1\partial_t\pi_2 - \pi_2\partial_t\pi_1) + \frac{1}{2}m_i^2\phi_i^2 + U(\langle\phi\rangle), \tag{2}$$

where $U(\langle\phi\rangle)$ is the classical potential, the meson mass m_i^2 generated by the condensates can be expressed as the second order derivative of $U(\phi)$ with respect to the meson field at $\phi = \langle\phi\rangle$, $m_i^2 = (\partial^2 U(\phi)/\partial\phi_i^2)|_{\phi=\langle\phi\rangle}$, and the interaction part $\mathcal{L}_{\rm int}$ contains three-meson and four-meson interactions with couplings in terms of the third and fourth order derivatives of $U(\phi)$.

The physical condensates $\langle\sigma\rangle$ and $\langle\pi_1\rangle$ are determined by the minimum potential

$$\frac{\partial U(\langle\phi\rangle)}{\partial\langle\sigma\rangle} = \langle\sigma\rangle(m^2 + \lambda(\langle\sigma\rangle^2 + \langle\pi_1\rangle^2)) - c = 0,$$
$$\frac{\partial U(\langle\phi\rangle)}{\partial\langle\pi_1\rangle} = \langle\pi_1\rangle(m^2 + \lambda(\langle\sigma\rangle^2 + \langle\pi_1\rangle^2) - \mu_I^2) = 0, \tag{3}$$

which guarantees the disappearance of the linear terms in σ and π in the interaction Lagrangian $\mathcal{L}_{\rm int}$.

The three model parameters, namely the mass parameter m^2, the four-meson coupling constant λ, and the chiral breaking parameter c, are fixed by fitting the meson masses $m_\pi^2 = m_{\pi_1}^2 = m_{\pi_2}^2 = m_{\pi_3}^2 = m^2 + \lambda\langle\sigma\rangle^2 = 135$ MeV and $m_\sigma^2 = m^2 + 3\lambda\langle\sigma\rangle^2 = 400$ MeV and the pion decay constant $f_\pi = \langle\sigma\rangle = 93$ MeV in vacuum. To guarantee the Lorentz invariance and parity conservation, the pion condensate should vanish in vacuum, $\langle\pi_1\rangle = 0$. At finite isospin chemical potential, the solution of the two coupled gap equations is $\langle\sigma\rangle = f_\pi, \langle\pi_1\rangle = 0$ in the normal phase at $\mu_I < m_\pi$ and $\langle\sigma\rangle = c/\mu_I^2, \langle\pi_1\rangle = \sqrt{(\mu_I^2 - m^2)/\lambda - c^2/\mu_I^4}$ in the pion superfluidity phase at $\mu_I > m_\pi$.

The inclusion of thermal excitations in the linear sigma model should be treated carefully. The Hartree-Fock approach is straightforward, but its disadvantage is the lack of the Goldstone mode in the symmetry breaking phase [29] at finite temperature and density. Here we introduce the thermal excitations through the large-N expansion [30] and focus on the phase diagram of pion superfluidity. Considering the $O(3)$ symmetry of the model in vacuum, we adopt the large-N expansion method in the $O(N)$ model with isospin chemical potential. With the same method and techniques given by Harber and Weldon [31], the condensates $\langle\sigma\rangle$ and $\langle\pi_1\rangle$ and the related mass parameter M^2 are controlled by the coupled gap equations

$$\langle\pi_1\rangle(M^2 - \mu_I^2) = 0,$$
$$\langle\sigma\rangle M^2 - c = 0,$$
$$M^2 = \lambda(\langle\pi\rangle^2 - f_\pi^2 + 2J'(T,\mu_I,M^2)) + \frac{c}{f_\pi}, \tag{4}$$

where the thermal excitations are included in the function $J'(T, \mu_I, M^2)$,

$$J' = \frac{1}{2}\int \frac{d^3\mathbf{p}}{(2\pi)^3}\frac{1}{E}(2f(E) + f(E-\mu_I) + f(E+\mu_I)) \quad (5)$$

with the quasiparticle energy $E = \sqrt{M^2 + \mathbf{p}^2}$ and Bose-Einstein distribution $f(x) = 1/(e^{x/T} - 1)$.

III. FRG APPLICATION TO PION SUPERFLUIDITY

We now apply the functional renormalization group to the SU(2) linear sigma model. The core quantity in the framework of FRG is the averaged effective action Γ_k at the RG scale k in Euclidean space, its scale dependence is described by the flow equation [14]

$$\partial_k \Gamma_k[\phi] = \frac{1}{2}\mathrm{Tr}(\partial_k R_k G_k[\phi]), \quad (6)$$

where the trace is performed in field space and momentum space, and $G_k[\phi]$ is the RG-modified propagator in field space,

$$G_k[\phi] = (\Gamma_k^{(2)} + R_k)^{-1}, \qquad \Gamma_k^{(2)} = \delta^2\Gamma_k/\delta\phi^2. \quad (7)$$

The evolution of the flow from ultraviolet limit $k = \Lambda$ to infrared limit $k = 0$ encodes, in principle, all the quantum and thermal fluctuations in the action. To suppress the fluctuations with momentum smaller than the scale k during the evolution, an infrared regulator R_k is introduced in the flow equation. At finite temperature and density where the Lorentz symmetry is broken, we employ the optimized regulator function $R_k(\mathbf{q}^2) = (k^2 - \mathbf{q}^2)\Theta(k^2 - \mathbf{q}^2)$, which is the three-dimensional analogue of the often used four-momentum regulator [32]. In order to solve the RG flow, a truncation is usually introduced and this, in principle, violates the regulator independence of the IR physics [33–36]. Under the truncation of local potential approximation (LPA), the optimized regulator is stable [37].

We take LPA to solve the flow equation (6) for the linear sigma model at finite isospin chemical potential, by truncating the effective action up to the order of ϕ^4,

$$\Gamma_k = \int d^4x\left[\frac{1}{2}(\partial_\mu\phi)^2 + i\mu_I(\pi_1\partial_t\pi_2 - \pi_2\partial_t\pi_1) + U_k(\phi)\right]. \quad (8)$$

Assuming uniform field configuration, the integral overspace and imaginary time is trivial, and the effective action $\Gamma_k = \beta V U_k$ is fully controlled by U_k, where V and $\beta = 1/T$ are the space and time region of the system. Since the $O(4)$ symmetry is broken by chiral and isospin symmetry breaking, the combination $\phi^2 = \sigma^2 + \boldsymbol{\pi}^2$ is no longer an invariant, instead, the effective potential has separate dependence on two invariants $\rho_\sigma = (\sigma^2 + \pi_0^2)/2$ and $\rho_\pi = (\pi_1^2 + \pi_2^2)/2$. With the explicit symmetry breaking, we have

$$U_k = m_k^2(\rho_\sigma + \rho_\pi) + \lambda_k(\rho_\sigma + \rho_\pi)^2 - \mu_I^2\rho_\pi - c\sigma. \quad (9)$$

A nonvanishing expectation κ_σ of ρ_σ signals chiral symmetry breaking and a nonvanishing expectation κ_π of ρ_π signals isospin symmetry breaking. They are determined by the stationary condition of the effective potential $\partial_\sigma U = \partial_{\pi_1} U = 0$, which gives

$$m_k^2(2\kappa_\sigma)^{1/2} + \lambda_k(2\kappa_\sigma)^{3/2} - c = 0, \qquad \kappa_\pi = 0 \quad (10)$$

in the normal phase without pion condensation and

$$\kappa_\sigma = \frac{c^2}{2\mu_I^4}, \qquad \kappa_\pi = \frac{\mu_I^2 - m_k^2}{2\lambda_k} - \frac{c^2}{2\mu_I^4} \quad (11)$$

in the pion superfluidity phase. These vacuum expectation values further serve as an expansion point when solving the flow equation for the effective potential.

The inverse propagator $G_k^{-1}[\phi]$ in field space defined by (7) has the following form,

$$G_k^{-1}[\phi] = \begin{pmatrix} K_\sigma & m_{\sigma\pi_1}^2 & 0 & 0 \\ m_{\sigma\pi_1}^2 & K_{\pi_1} & 2\mu_I\omega_n & 0 \\ 0 & -2\mu_I\omega_n & K_{\pi_2} & 0 \\ 0 & 0 & 0 & K_{\pi_0} \end{pmatrix} \quad (12)$$

with

$$\begin{aligned} K_\sigma &= \omega_n^2 + \mathbf{q}_R^2 + m_\sigma^2, \\ K_{\pi_0} &= \omega_n^2 + \mathbf{q}_R^2 + m_{\pi_0}^2, \\ K_{\pi_1} &= \omega_n^2 + \mathbf{q}_R^2 + m_{\pi_1}^2 - \mu_I^2, \\ K_{\pi_2} &= \omega_n^2 + \mathbf{q}_R^2 + m_{\pi_2}^2 - \mu_I^2, \\ m_\sigma^2 &= U_k^{(1,0)} + 2\rho_\sigma U_k^{(2,0)}, \\ m_{\pi_0}^2 &= U_k^{(1,0)}, \\ m_{\pi_1}^2 &= U_k^{(0,1)} + 2\rho_\pi U_k^{(0,2)}, \\ m_{\pi_2}^2 &= U_k^{(0,1)}, \\ m_{\sigma\pi_1}^2 &= 2\sqrt{\rho_\sigma\rho_\pi}U_k^{(1,1)}, \end{aligned} \quad (13)$$

where $\mathbf{q}_R^2 = \mathbf{q}^2 + R_k(\mathbf{q}^2)$ is the RG-modified momentum, $\omega_n = 2n\pi T$ with $n = 0, \pm1, \pm2, \cdots$ are the Matsubara frequencies of bosons, and $U_k^{m,n}$ are the derivatives of the potential with respect to ρ_σ and ρ_π,

$$U_k^{(m,n)} = \frac{\delta^{(m+n)}}{\delta\rho_\sigma^m \delta\rho_\pi^n} U_k. \tag{14}$$

In the normal phase with $\kappa_\pi = 0$, there is no mixture between σ and π_1; the propagator is simplified as

$$G_k[\phi] = \begin{pmatrix} G_\sigma & 0 & 0 & 0 \\ 0 & G_{\pi_1} & -G_{\pi_1\pi_2} & 0 \\ 0 & G_{\pi_1\pi_2} & G_{\pi_2} & 0 \\ 0 & 0 & 0 & G_{\pi_0} \end{pmatrix} \tag{15}$$

with

$$\begin{aligned} G_\sigma &= 1/K_\sigma, \\ G_{\pi_0} &= 1/K_{\pi_0}, \\ G_{\pi_1} &= K_{\pi_2}/J, \\ G_{\pi_2} &= K_{\pi_1}/J, \\ G_{\pi_1\pi_2} &= 2\mu_I\omega_n/J, \\ J &= 4\mu_I^2\omega_n^2 + K_{\pi_1}K_{\pi_2}. \end{aligned} \tag{16}$$

In the pion superfluid phase, there is a mixture in $\sigma - \pi_1 - \pi_2$ subspace; the propagator becomes

$$G_k[\phi] = \begin{pmatrix} G_\sigma & -G_{\sigma\pi_1} & G_{\sigma\pi_2} & 0 \\ -G_{\sigma\pi_1} & G_{\pi_1} & -G_{\pi_1\pi_2} & 0 \\ -G_{\sigma\pi_2} & G_{\pi_1\pi_2} & G_{\pi_2} & 0 \\ 0 & 0 & 0 & G_{\pi_0} \end{pmatrix} \tag{17}$$

with

$$\begin{aligned} G_\sigma &= (4\mu_I^2\omega_n^2 + K_{\pi_1}K_{\pi_2})/J, \\ G_{\pi_0} &= 1/K_{\pi_0}, \\ G_{\pi_1} &= K_\sigma K_{\pi_2}/J, \\ G_{\pi_2} &= (K_\sigma K_{\pi_1} - m_{\sigma\pi_1}^4)/J, \\ G_{\sigma\pi_1} &= m_{\sigma\pi_1}^2 K_{\pi_2}/J, \\ G_{\sigma\pi_2} &= 2\mu_I\omega_n m_{\sigma\pi_1}^2/J, \\ G_{\pi_1\pi_2} &= 2\mu_I\omega_n K_\sigma(q)/J, \\ J &= K_\sigma(K_{\pi_1}K_{\pi_2} + 4\mu_I^2\omega_n^2) - m_{\sigma\pi_1}^4 K_{\pi_2}. \end{aligned}$$

By putting these propagators into the flow equation (6), taking the momentum integration with optimized regulator function R_k, and performing the Matsubara frequency summation, we obtain the flow equation for the effective potential

$$\partial_k U_k = \frac{1}{2} I_\sigma(0) + \frac{1}{2} I_{\pi_0}(0) + \frac{1}{2}\sum_\pm I_{\pi_\pm}(\pm\mu_I) \tag{18}$$

in the normal phase and

$$\partial_k U_k = \frac{1}{2} I_{\pi_0}(0) + \frac{1}{2}\sum_{j\in\{\Sigma,\Pi_1,\Pi_2\}} R_j I_j(0) \tag{19}$$

in the superfluidity phase, where

$$I_i(\mu) = \frac{k^4}{3\pi^2}\frac{1+2n_B(E_i+\mu)}{2E_i} \tag{20}$$

is the loop function for quasiparticles with energy E_i and occupation number

$$n_B(E) = \frac{1}{e^{E/T}-1}. \tag{21}$$

Note that, due to the spontaneous isospin symmetry breaking in the superfluidity phase, σ, π_1, and π_2 are no longer the eigenstates of the Hamiltonian of the system. The new eigenmodes Σ, Π_1, Π_2 are linear combinations of σ, π_1, π_2 and their masses m_j with $j \in \{\Sigma, \Pi_1, \Pi_2\}$ are determined by the three poles of the meson propagator (17). The coefficients R_j in (19) are the corresponding residues at the three poles.

With two condensates in field space, there are several evaluation methods to solve the flow equation: one- and two-dimensional Taylor expansion with running minimum [38,39], Taylor expansion about a fixed background [40] and a grid of field [41]. Similar to the method in [39], we adopt here a two-dimensional Taylor expansion by expanding $U_k(\rho_\sigma, \rho_\pi)$ at the running minimum $(\kappa_\sigma, \kappa_\pi)$ to the second order. Considering that the main physics is spontaneous chiral symmetry breaking in the normal phase and spontaneous isospin symmetry breaking in the pion superfluidity phase, we neglect the fluctuations in the pion condensate in the normal phase and fluctuations in the chiral condensate in the pion superfluidity phase. This approximation reduces the dimension of the expansion from 2 to 1 and and largely simplifies the structure of the flow equations. Under this approximation, in the normal phase with $\rho_\pi = 0$, the effective potential becomes a function of $O(4)$ invariant $\rho = \rho_\sigma$. The running minimum k_σ is the solution to the stationary condition (10). Taking into account the stationary condition $m_k^2 = -2\lambda_k\kappa_\sigma + c/\sqrt{2\kappa_\sigma}$ and its scale derivative $\partial_k m_k^2 = -2\kappa_\sigma\partial_k\lambda_k - (2\lambda_k + c/(2\kappa_\sigma)^{3/2})\partial_k\kappa_\sigma$, the flow equation in the normal phase can be rewritten as

$$\partial_k U_k = \frac{c}{(2\kappa_\sigma)^{3/2}}\partial_k\kappa_\sigma(\rho-\kappa_\sigma) + \partial_k\lambda_k(\rho-\kappa_\sigma)^2. \tag{22}$$

There should be a constant term in the expansion that is the potential at the running minimum $U(\kappa_\sigma)$ and only related to the thermal properties of the system. Since we focus on the critical properties of the system, we have dropped this constant part.

In the superfluid phase, the minimum κ_σ is scale independent and can be treated as a background field. Under the approximation of neglecting fluctuations in ρ_σ, we expand the effective potential at the running minimum $\kappa = \kappa_\sigma + \kappa_\pi$. With the stationary condition in the superfluid phase, the scale derivative of the effective potential can be reparametrized in the superfluid phase,

$$\partial_k U_k = \left(\partial_k m_k^2 + \frac{\mu_I^2 - m_k^2}{\lambda_k}\partial_k\lambda_k\right)(\rho-\kappa) + \partial_t\lambda_k(\rho-\kappa)^2. \tag{23}$$

In both phases, the flow equations for the parameters m_k^2 and λ_k are obtained by expanding the right-hand side of (18) or (19) to the second order at the corresponding running minimum (10) or (11) and then comparing the coefficients with (22) or (23).

IV. NUMERICAL RESULTS

In this section we numerically solve the two coupled flow equations and show our results for the phase diagram of pion superfluidity and the corresponding critical exponents at finite temperature and isospin chemical potential. With the help of the explicit solutions (10) and (11) for the condensates, the initial condition for the two flow equations at fixed temperature and chemical potential is the values of the mass and coupling parameters $m_\Lambda^2(T,\mu_I)$ and $\lambda_\Lambda(T,\mu_I)$ at the ultraviolet momentum Λ and the k-independent parameter c controlling the degree of explicit chiral symmetry breaking. In principle, the initial condition of the flow in low-energy effective models should be obtained by integrating the QCD flow equation down to the scale Λ. Considering the fact that the system at extremely high momentum should be dominated by the dynamics and not affected remarkably by the external parameters like temperature and chemical potential, we take, as a first order approximation, temperature and chemical potential independent initial values $m_\Lambda^2(T,\mu_I) = m_\Lambda^2(0,0)$ and $\lambda_\Lambda(T,\mu_I) = \lambda_\Lambda(0,0)$ in the following numerical calculation. Their values are so chosen to fit the meson masses and pion decay constant in vacuum at the infrared limit. Their values are listed in Table I.

TABLE I. The initial parameters m_Λ^2 and λ_Λ at the UV limit and c by fitting the meson masses and pion decay constant in vacuum at the infrared limit. The cutoff is set to be $\Lambda = 800$ MeV and m_π, m_σ, and f_π are given in MeV.

m_Λ^2/Λ^2	λ_Λ	c/Λ^3	f_π	m_π	m_σ
−0.4453	16.93	0.0033	93.02	134.98	400.43

How to choose the value of the ultraviolet scale Λ should be carefully discussed in effective models. In models with hadrons as elementary constituents, the momentum scale cannot go beyond the scale of the model itself where the hadrons are well defined. This means that the momentum scale should be restricted in a reasonable region. In the following calculation we take $\Lambda = 800$ MeV for the starting point of the evolution of the renormalization parameters. We have checked that the physical results at $k = 0$ are not sensitive to the further increased Λ. With the given initial condition, the two flow equations are solved by the fourth order Runge-Kutta method with step length $dk = 10^{-4}$ MeV. We reach the infrared scale $k_{\rm min} < 10^{-3}$ MeV.

In vacuum, the evolution of the mass and coupling parameters m_k^2 and λ_k and the chiral condensate $\langle\sigma\rangle_k$ with RG scale k is shown in Fig. 1. They all drop down rapidly in the beginning and become saturated at $k \to 0$, guaranteeing the stability of the flow equations in the infrared limit.

The increasing condensate with scale in meson models, as shown in Fig. 1 and [42] and [43], looks suspicious, as in one-flavor QCD [44] and quark-meson models [45] the chiral condensate drops down with increasing scale and approaches 0 when the UV scale is high enough. This difference may come from the sign $\pm$ on the right-hand side of the flow equations $\partial_k\Gamma_k = +(1/2)\mathrm{Tr}(\partial_k R_k G_k)$ for bosons and $\partial_k\Gamma_k = -\mathrm{Tr}(\partial_k R_k G_k)$ for fermions. Since $\partial_k R_k G_k$ is positively definite, the sign $\pm$ leads to an increasing potential for mesons and decreasing potential for quarks. For systems with both quark and meson degrees of freedom, the UV limit is controlled by quarks. Note that, while the evolution process of the flow from ultraviolet limit to infrared limit is different for meson and quark systems, both can reach the correct infrared limit by choosing suitable initial conditions.

The chiral and pion condensations at finite temperature and isospin chemical potential are displayed and compared

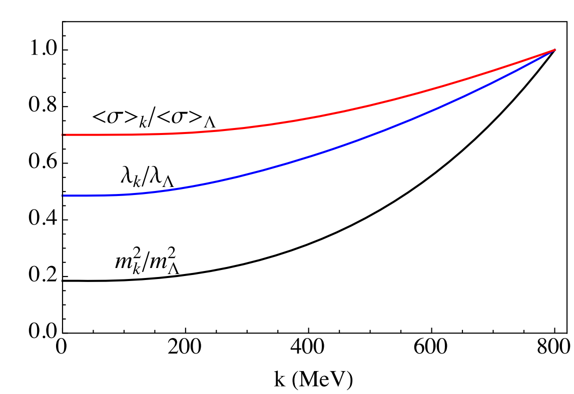

FIG. 1. The evolution of the scaled mass parameter m_k^2/m_Λ^2, coupling constant $\lambda_k/\lambda_\Lambda$, and chiral condensate $\langle\sigma\rangle_k/\langle\sigma\rangle_\Lambda$ with RG scale k in vacuum.

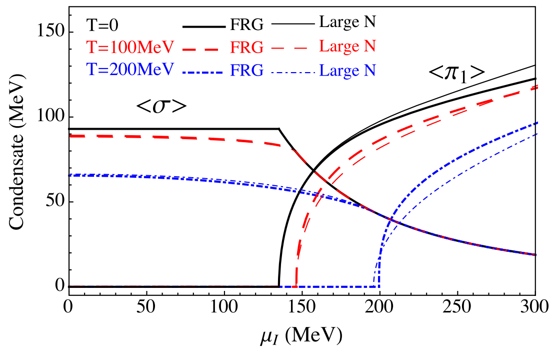

FIG. 2. The chiral and pion condensates $\langle\sigma\rangle$ and $\langle\pi_1\rangle$ as functions of isospin chemical potential at different temperatures in the FRG and large-N expansion approaches.

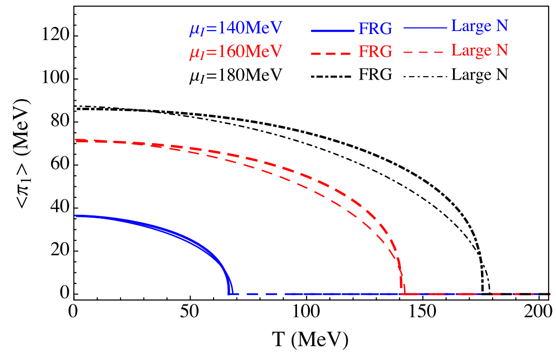

FIG. 3. The pion condensate $\langle\pi_1\rangle$ as a function of temperature at different isospin chemical potential in the FRG and large-N expansion approaches.

with the large-N expansion in Fig. 2. The system is in normal phase at low isospin chemical potential and enters the pion superfluidity phase at the critical isospin chemical potential $\mu_I^c = m_\pi$. Because of the explicit chiral symmetry breaking ($c \neq 0$), the chiral condensate does not disappear in the superfluidity phase. While there is almost no difference between the FRG and large-N expansion for the chiral condensate, the difference is remarkable for the pion condensate. Especially, the critical isospin chemical potentials in the two approaches do not coincide at high temperature.

At mean field level, the critical isospin chemical potential $\mu_I^c = m_\pi$ can be analytically obtained by combining the gap equation (11) and the pion mass in vacuum $m_\pi^2 = m^2 + \lambda\sigma^2$. When the fluctuations are included, it is not trivial to keep this critical value in the FRG framework. In quark-meson model [11], it is largely violated when taking the pion screening mass as the physical mass. The violation can be cured by properly feeding the momentum dependent propagators back into the flow equation for the effective potential [11,41]. In boson models the violation becomes much weaker even at LPA level [46]. In our treatment the critical value $\mu_I^c = m_\pi$ comes from the one-dimensional Taylor expansions (22) for normal matter and (23) for pion superfluidity. Since the $O(4)$ symmetry is broken by chiral condensation and nonzero isospin chemical potential, the combination $\rho = \rho_\sigma + \rho_\pi$ is no longer an invariant, the effective potential depends separately on ρ_σ and ρ_π, and its expansion should be two dimensional. In our treatment, however, we have neglected the fluctuations in ρ_π in normal phase and in ρ_σ in pion superfluidity. Under this approximation, the expansions (22) and (23) become one dimensional, which keeps the condition $\mu_I^c = m_\pi$. The result here is similar to the conclusion in Ref. [39] with one-dimensional expansion. While the fluctuations in ρ_σ (ρ_π) are the dominant fluctuations in normal matter (pion superfluidity), a two-dimensional expansion in ρ_σ and ρ_π is expected to violate the condition $\mu_I^c = m_\pi$.

The difference between the large-N and FRG approaches in the pion superfluidity can also be seen in Fig. 3. Again, the temperature and chemical potential behavior of the pion superfluidity, especially the location of the critical temperature, depends on the used approaches. Note that, while the difference in the critical temperature and chemical potential is small, it may significantly change the critical exponents; see the following discussion.

For a continuous phase transition, while the temperature and chemical potential dependence of the order parameter and the location of the phase transition line are related to the detailed dynamics of the used model, the critical behavior of the phase transition is controlled only by the symmetry and the space-time dimension of the system. In the vicinity of a continuous phase transition, fluctuations become dominant and the correlation length approaches infinity. In this case, the difference between the FRG that focuses on quantum and thermal fluctuations and the large-N expansion can be clearly understood from the perspective of critical exponents. From the scaling laws, $\gamma = \beta(\delta - 1)$, $\alpha + 2\beta + \gamma = 2$, $d\nu = 2 - \alpha$ and $\gamma = \nu(2 - \eta)$, only two among the six critical exponents are independent. Since we have taken local potential approximation, the anomalous dimension disappears, $\eta = 0$, and we have only one independent critical exponent.

For the phase transition of pion superfluidity, the critical exponent β describing the behavior of the order parameter $\langle\pi_1\rangle$ is defined as

$$\langle\pi_1\rangle \sim \left(\frac{T_c - T}{T_c}\right)^\beta. \tag{24}$$

In Tables II and III we show the critical isospin chemical potential μ_I^c and critical exponent β at temperature T in the

TABLE II. The critical isospin chemical potential μ_I^c and critical exponent β at temperature T, calculated in the FRG approach.

T(MeV)	0	10	50	100	150	200	250
μ_I^c(MeV)	135.0	135.2	138.0	146.3	164.5	199.4	248.9
β	0.5	0.445	0.380	0.347	0.328	0.318	0.314

TABLE III. The critical isospin chemical potential μ_I^c and critical exponent β at temperature T, calculated in the large-N expansion approach.

T(MeV)	0	10	50	100	150	200	250
μ_I^c(MeV)	135.0	135.2	137.8	146.0	163.5	195.9	242.5
β	0.5	0.5	0.5	0.5	0.5	0.5	0.5

FRG and large-N expansion approaches. From the comparison of the two methods, the big difference lies in the critical exponent β which is controlled by fluctuations. With the large-N expansion, β is temperature independent and keeps its mean field value 0.5. In the framework of FRG, however, β decreases continuously from 0.5 to 0.313 with increasing temperature. In the beginning it drops down rapidly and then becomes saturated when the temperature is high enough.

The calculation of the critical exponents does not depend on the path approaching the phase transition point in the $T-\mu_I$ plane, since the correlation length goes to infinity in any direction moving to the transition point. In the above calculation of β, μ_I is kept as a constant and the path is parallel to the T axis. We checked the calculation with the path parallel to the μ_I axis, namely, taking $\langle\pi_1\rangle\sim((\mu_I-\mu_I^c)/\mu_I^c)^\beta$, the result is the same as with (24).

V. A COMPAISON: $O(N)$ MODEL IN CONTINUOUS DIMENSION

The critical properties of a continuous phase transition at finite temperature and density can alternatively be described by space-time dimension reduction in vacuum. In finite temperature field theory [47,48], the imaginary time corresponds to the inverse temperature of the system T^{-1}. The two length scales of the system defined in the Euclidean space $S^1\times R^{d-1}$ can be the circumference T^{-1} of S^1 and the inverse RG scale k^{-1} for R^{d-1}. The space-time integration at finite temperature becomes

$$\int_0^\infty d^dx \to \int_0^{T^{-1}} dt\int_0^\infty d^{d-1}\mathbf{x}. \tag{25}$$

In low temperature limit $T\to 0$, the integration over time is from 0 to ∞, and the space-time dimension is d. In high temperature limit $T\to\infty$, however, the time integration vanishes; the dimension of the system drops from d of $S^1\times R^{d-1}$ to $d-1$ of R^{d-1}. Between the low and high temperature limits, the effective dimension of the system d_{eff} changes continuously from d to $d-1$.

To show the fact that the critical exponents calculated above are independent of the details of the pion superfluidity in the linear sigma model but controlled only by the symmetry and the space-time dimension of the system, we recalculate in this section the critical exponents in a simpler model with intrinsic symmetry $O(N)$ and continuous dimension $3<d<4$ in vacuum. With different N, the $O(N)$ model is able to capture the symmetry of different systems [49], and with varying dimension d, the model can provide a deep insight into the critical phenomenon of low dimension systems with $d<3$ [50] and of high dimensional systems with $d>4$ [49,51,52]. The critical exponents are discussed in the $O(N)$ model at fixed dimension $d=3$ [35]. What we focus on here is their dimension dependence and dimension reduction.

The Euclidean Lagrangian density of the model involves a set of N real scalar fields $\phi_i,(i=1,\ldots,N)$,

$$\mathcal{L}_N=\frac{1}{2}\partial_\mu\phi_i\partial^\mu\phi_i+U(\phi^2) \tag{26}$$

with the effective potential

$$U(\phi^2)=\frac{1}{2}a\phi_i\phi_i+\frac{1}{4}b(\phi_i\phi_i)^2, \tag{27}$$

where a and b are respectively the mass parameter and coupling constant. Suppose one of the N components is with finite vacuum expectation value $\langle\phi_j\rangle$; the Goldstone theorem guarantees $N-1$ massless particles. Defining the invariant of the system $\rho=\phi_j^2/2$ and making a shift $\phi_j\to\langle\phi_j\rangle+\phi_j$, we obtain the flow equation for the effective potential,

$$\partial_k U_k=S_d k^{d+1}\left[\frac{1}{k^2+U_k'+2\rho U_k''}+\frac{N-1}{k^2+U_k'}\right], \tag{28}$$

where $U_k(\phi^2)$ is $U(\phi^2)$ but with k-dependent parameters a_k and b_k, $U_k'+2\rho U_k''$ is the squared curvature mass of ϕ_j with $U_k'=\partial U_k/\partial\rho$ and $U_k''=\partial^2U_k/\partial\rho^2$. Note that the mass U_k' of $N-1$ Goldstone particles is guaranteed to be 0 by the gap equation.

By expanding the flow equation around the classical fields, comparing the linear and quadratic terms on the both sides, and taking into account the gap equation $\partial U_k/\partial\langle\phi_j\rangle=0$ that leads to only two independent parameters a_k and b_k, the flow equation for U_k is converted into two coupled flow equations for a_k and b_k. Then we introduce the dimensionless parameters,

$$\bar{a}_k=k^{-2}a_k,\qquad \bar{b}_k=k^{d-4}b_k; \tag{29}$$

the flow equations for $\bar{a}_k$ and $\bar{b}_k$ can be explicitly expressed as

$$\begin{aligned}\partial_t\bar{a}_t&=-2\bar{a}_t-2S_d\bar{b}_t\\&\quad\times\left[\left(\frac{3}{E_1^4}+\frac{N-1}{E_2^4}\right)-2\bar{a}_t\left(\frac{9}{E_1^6}+\frac{N-1}{E_2^6}\right)\right],\\ \partial_t\bar{b}_t&=(d-4)\bar{b}_t+4S_d\bar{b}_t^2\left(\frac{9}{E_1^6}+\frac{N-1}{E_2^6}\right)\end{aligned} \tag{30}$$

with the RG time $t = \ln(k/\Lambda)$, the phase space factor $S_d = 1/(d2^{d-1}\pi^{d/2}\Gamma(d/2))$, and the dimensionless energies $E_1 = \sqrt{1-2\bar{a}_k}$ for the massive particle ϕ_j and $E_2 = 1$ for the $N-1$ Goldstone particles ϕ_i. Giving an arbitrary initial condition $\bar{a}_0$ and $\bar{b}_0$ at $t = 0$, we can solve the flow equations and obtain an evolution curve in the parameter plane $(\bar{a}_t, \bar{b}_t)$, and the collection of all the curves forms the flow diagram. From the definition, the fixed points of the flow are characterized by the equations

$$\begin{aligned} 0 &= 2\bar{a}_t + 2S_d\bar{b}_t \\ &\quad\times\left[\left(\frac{3}{E_1^4}+\frac{N-1}{E_2^4}\right) - 2\bar{a}_t\left(\frac{9}{E_1^6}+\frac{N-1}{E_2^6}\right)\right], \\ 0 &= (d-4)\bar{b}_t + 4S_d\bar{b}_t^2\left(\frac{9}{E_1^6}+\frac{N-1}{E_2^6}\right). \end{aligned} \tag{31}$$

Figure 4 shows the flow diagrams of the $O(2)$ model in the dimensionless parameter plane $(\bar{a}_t, \bar{b}_t)$ at different dimensions $d = 3, 3\frac{1}{3}, 3\frac{2}{3}$, and 4 from top to bottom. When the dimension d increases from 3 to 4, there exist both the Wilson-Fisher fixed point and Gaussian fixed point, and the critical behavior of the phase transition at finite temperature is governed by the Wilson-Fisher fixed point. With increasing dimension, the Gaussian fixed point is always located at $(\bar{a}_t, \bar{b}_t) = (0, 0)$, and the Wilson-Fisher fixed point approaches it continuously and finally merges with it at $d = 4$. At $d = 4$, the Gaussian fixed point becomes a mixed one with flows going in and out and governs the critical behavior of the system.

With the standard procedure of renormalization group [23], by linearizing the flow equations (30) in the vicinity of the Wilson-Fisher fixed point (Gaussian fixed point at $d = 4$) and calculating the eigenvalues of the Jacobian, we can accordingly obtain the critical exponent ν describing the singularity in the correlation length. Using the scaling law $\beta = (d-2)/2\nu$ we can further find the critical exponent β. The result for $O(N)$ models with different N in continuous dimension between 3 and 4 is listed in Table IV.

At $d = 4$, the critical exponents are characterized by the Gaussian fixed point of a free boson system, and the fluctuations could be neglected in the vicinity of the critical point. When the dimension is slightly less than 4, the Wilson-Fisher fixed point is very close to the Gaussian fixed point, the system is in a weakly coupled state, and the perturbation expansion is self-consistent in this region. From the expansion in terms of $4-\epsilon$, the critical exponent ν can be simplified as $\nu^{-1} = 2 - (N+2)/(N+8)\epsilon$ for small ϵ. When ϵ is not small enough, the Wilson-Fisher point is far from the Gaussian fixed point, the system around the phase transition is in a strongly coupled state, and nonperturbative approaches are required to deal with the dominant fluctuations.

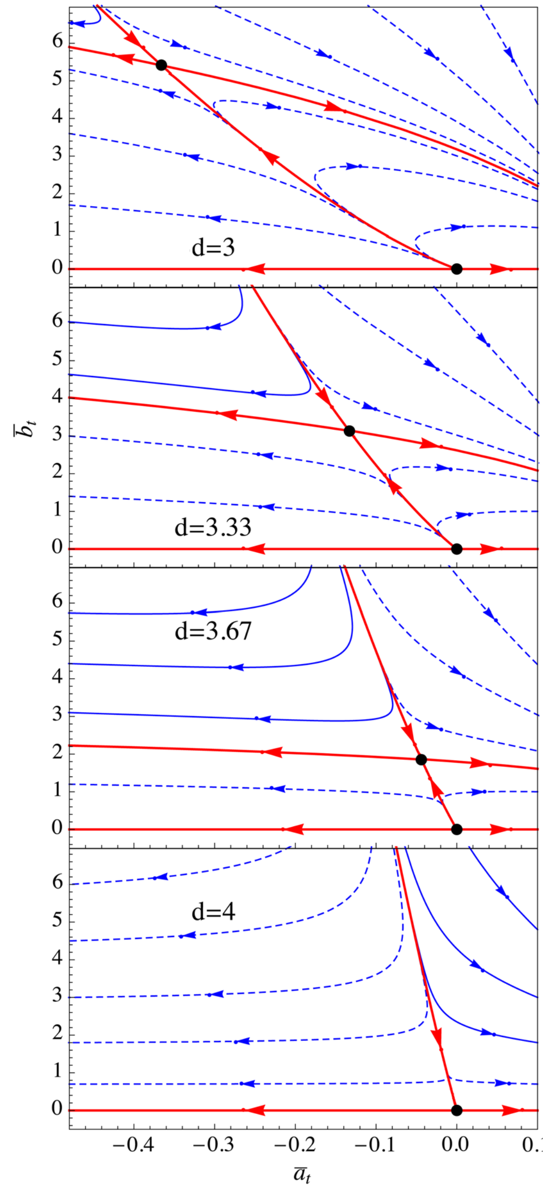

FIG. 4. The flow diagrams of the $O(2)$ model in the dimensionless parameter plane $(\bar{a}_t, \bar{b}_t)$ at dimension $d = 3, 3\frac{1}{3}, 3\frac{2}{3}$, and 4 from top to bottom.

We now compare the critical exponents calculated from the fixed point analysis in the $O(N)$ model with continuous dimension and from linearly fitting the pion condensates in FRG and large-N expansion approaches. As shown in

TABLE IV. The critical exponent β calculated in $O(N)$ models with continuous dimension $3 \le d \le 4$.

	d							
N	3	3.1	3.2	3.4	3.6	3.8	3.9	4
$O(2)$	0.311	0.328	0.349	0.394	0.434	0.469	0.485	0.5
$O(3)$	0.365	0.368	0.378	0.409	0.442	0.472	0.486	0.5
$O(4)$	0.398	0.397	0.401	0.421	0.448	0.474	0.487	0.5
$O(\infty)$	0.5	0.5	0.5	0.5	0.5	0.5	0.5	0.5

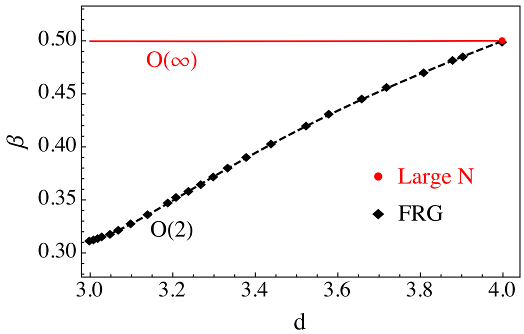

FIG. 5. The critical exponent β as a function of continuous dimension d. The solid and dashed lines are the calculations in $O(\infty)$ and $O(2)$ models, and the dot and diamonds are the results of pion superfluidity in large-N expansion and FRG approaches.

Fig. 5, solid and dashed lines are the $O(\infty)$ and $O(2)$ model calculations. Since the critical exponents are controlled by the symmetry and space-time dimension of the system only and not sensitive to the detailed dynamics, namely, the superfluidity or the general $O(2)$-type dynamics, there should be the relation between the calculations at finite temperature and continuous dimension,

$$\beta(T_c) = \beta(d_c). \tag{32}$$

The dot and diamonds in Fig. 5 are the values of β calculated with dynamics of pion superfluidity in large-N expansion and FRG approaches shown in Sec. IV. From the relation (32) we can extract the critical dimension corresponding to the critical temperature $d_c(T_c)$ that is demonstrated in Fig. 6. The critical dimension decreases continuously from 4 to 3 with increasing critical temperature from 0 to the maximum value ~300 MeV.

Including baryon chemical potential μ_B in the calculation of pion superfluidity in QCD and effective models like NJL and quark-meson models, the pion condensate is reduced by the imbalance between the Fermi surfaces of u and $\bar{d}$ quarks, and the critical temperature becomes lower than the one shown in Table II. In this case, the line $T_c(d_c)$ at a nonzero μ_B, extracted from the relation $\beta(T_c, \mu_B) = \beta(d_c)$,

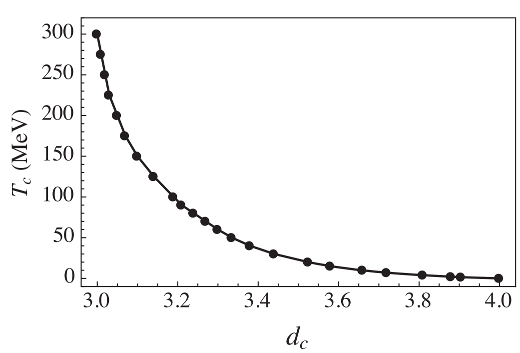

FIG. 6. The relation between critical temperature and critical dimension, from the comparison between pion superfluidity at finite temperature and $O(2)$ model with continuous dimension.

starts at a lower temperature in comparison with the one shown in Fig. 6 at $\mu_B = 0$.

The Taylor expansion around the running minimum is a usually used way to solve FRG flow equations, with which one can explicitly see the evolution of the coupling parameters under the scale transformation. However, the speed of convergence of the expansion depends on the model used. For $O(N)$ models with $N \leq 4$, a good convergence of the critical exponents needs the expansion to at least the third order, as discussed in [35]. When N is large enough, the convergence is already good enough with the expansion to the second order. In our treatment for the pion superfluidity in the linear sigma model, we expanded the flow equation only to the second order. It is expected that including the higher order contribution to the flow equation may change the values of the critical exponents. However, since the expansions in both the linear sigma model and $O(2)$ model are at the same order, the relation between the critical temperature and dimension extracted from the comparison of the two models may not be so sensitive to the higher order correction. As for the large-N approach, there is already a big difference from the FRG approach, shown in Tables II and III for the critical exponent; the higher order contribution does not qualitatively modify the difference.

VI. SUMMARY

We studied the critical behavior of pion superfluidity at finite temperature and isospin chemical potential and its relation to the dimension crossover at zero temperature. In the framework of functional renormalization group, we calculated the critical exponents of the pion superfluidity in the SU(2) linear sigma model at finite temperature and isospin density and compared them with a general $O(N)$ model at zero temperature and density. The pion superfluidity is a second order phase transition driven by isospin density. At zero temperature, the critical exponents $\beta = 0.5$ for the order parameter correspond to the four-dimensional $O(2)$ universality class. When temperature is turned on, the critical exponent β changes with temperature, and the phase transition corresponds to a $O(2)$ universality class with a dimension crossover from $d = 4$ to $d = 3$. In the limit of high temperature, the critical exponent is saturated at $\beta = 0.31$, corresponding to the three-dimensional $O(2)$ universality class.

We also compared the FRG with large-N expansion in the linear sigma model. The two approaches give the same critical behavior only at zero temperature where thermal fluctuations are negligible in the vicinity of the phase transition. This agreement is predicted by the Ginzburg criterion [22] that $d = 4$ is the upper critical dimension of the mean field approach. From the perspective of FRG, the critical phenomenon at $d = 4$ is governed by the Gaussian fixed point, around which the system is reduced to a weakly coupled one, justifying the self-consistency of mean field treatment and

$4-\epsilon$ expansion. Turning on the temperature, the difference between the two approaches becomes obvious. For dimension much less than 4, fluctuations in the critical region play the dominant role. The large-N expansion and perturbation treatment are no longer self-consistent; nonperturbative treatments of fluctuations are required.

ACKNOWLEDGMENTS

We thank Yin Jiang for helpful discussions during the work. The work is supported by the NSFC and MOST Grants No. 11335005, No. 11575093, No. 2013CB922000, and No. 2014CB845400.

[1] S. Barshay and G. E. Brown, Phys. Lett. **47B**, 107 (1973).
[2] V. A. Khodel, J. W. Clark, M. Takano, and M. V. Zverev, Phys. Rev. Lett. **93**, 151101 (2004).
[3] J. B. Kogut and D. K. Sinclair, Phys. Rev. D **66**, 034505 (2002).
[4] J. B. Kogut and D. K. Sinclair, Phys. Rev. D **70**, 094501 (2004).
[5] P. de Forcrand, M. A. Stephanov, and U. Wenger, *Proc. Sci.*, LAT2007 (2007) 237.
[6] W. Detmold, K. Orginos, and Z. Shi, Phys. Rev. D **86**, 054507 (2012).
[7] G. Endrödi, Phys. Rev. D **90**, 094501 (2014).
[8] B. Klein, D. Toublan, and J. J. M. Verbaarschot, Phys. Rev. D **68**, 014009 (2003).
[9] B. Klein, D. Toublan, and J. J. M. Verbaarschot, Phys. Rev. D **72**, 015007 (2005).
[10] L. He, M. Jin, and P. Zhuang, Phys. Rev. D **71**, 116001 (2005).
[11] K. Kamikado, N. Strodthoff, L. von Smekal, and J. Wambach, Phys. Lett. B **718**, 1044 (2013).
[12] E. E. Svanes and J. O. Andersen, Nucl. Phys. **A857**, 16 (2011).
[13] T. H. Phat and N. V. Thu, J. Phys. G **38**, 045002 (2011).
[14] J. Berges, N. Tetradis, and C. Wetterich, Phys. Rep. **363**, 223 (2002).
[15] H. Gies, Lect. Notes Phys. **852**, 287 (2012).
[16] C. S. Fischer, A. Maas, and J. M. Pawlowski, Ann. Phys. (Amsterdam) **324**, 2408 (2009).
[17] M. Mitter, J. M. Pawlowski, and N. Strodthoff, Phys. Rev. D **91**, 054035 (2015).
[18] T. Appelquist and R. D. Pisarski, Phys. Rev. D **23**, 2305 (1981).
[19] For instance, see J. L. Hewett and M. Spiropulu, Annu. Rev. Nucl. Part. Sci. **52**, 397 (2002); G. 't Hooft, arXiv:gr-qc/9310026; O. Lauscher and M. Reuter, Phys. Rev. D **65**, 025013 (2001); T. Appelquist and A. Chodos, Phys. Rev. D **28**, 772 (1983).
[20] S. B. Liao and M. Strickland, Nucl. Phys. **B497**, 611 (1997).
[21] H. Ballhausen, J. Berges, and C. Wetterich, Phys. Lett. B **582**, 144 (2004).
[22] J. Als-Nielsen and R. J. Birgeneau, Am. J. Phys. **45**, 554 (1977).
[23] K. G. Wilson and M. E. Fisher, Phys. Rev. Lett. **28**, 240 (1972).
[24] R. Guida and J. Zinn-Justin, J. Phys. A **31**, 8103 (1998).
[25] Y. Nemoto, K. Naito, and M. Oka, Eur. Phys. J. A **9**, 245 (2000).
[26] J. Baacke and S. Michalski, Phys. Rev. D **67**, 085006 (2003).
[27] J. O. Andersen and T. Brauner, Phys. Rev. D **78**, 014030 (2008).
[28] J. O. Andersen, D. Boer, and H. J. Warringa, Phys. Rev. D **70**, 116007 (2004).
[29] N. Petropoulos, arXiv:hep-ph/0402136.
[30] M. Moshe and J. Zinn-Justin, Phys. Rep. **385**, 69 (2003).
[31] H. E. Haber and H. A. Weldon, Phys. Rev. D **25**, 502 (1982).
[32] D. F. Litim, Phys. Lett. B **486**, 92 (2000).
[33] R. D. Ball, P. E. Haagensen, J. Latorre, and E. Moreno, Phys. Lett. B **347**, 80 (1995).
[34] D. F. Litim, Phys. Rev. D **64**, 105007 (2001).
[35] D. F. Litim, Nucl. Phys. **B631**, 128 (2002).
[36] D. F. Litim, J. High Energy Phys. 07 (2005) 005.
[37] J. M. Pawlowski, Ann. Phys. (Amsterdam) **322**, 2831 (2007).
[38] K. Kamikado and T. Kanazawa, J. High Energy Phys. 01 (2015) 129.
[39] N. Khan, J. M. Pawlowski, F. Rennecke, and M. M. Scherer, arXiv:1512.03673.
[40] J. M. Pawlowski and F. Rennecke, Phys. Rev. D **90**, 076002 (2014).
[41] N. Strodthoff, B. J. Schaefer, and L. von Smekal, Phys. Rev. D **85**, 074007 (2012).
[42] O. Bohr, B. J. Schaefer, and J. Wambach, Int. J. Mod. Phys. **A16**, 3823 (2001).
[43] Y. Jiang and P. Zhuang, Phys. Rev. D **86**, 105016 (2012).
[44] H. Gies and C. Wetterich, Phys. Rev. D **69**, 025001 (2004).
[45] J. Braun, B. Klein, and H.-J. Pirner, Phys. Rev. D **71**, 014032 (2005).
[46] K. Kamikado, N. Strodthoff, L. von Smekal, and J. Wambach, Eur. Phys. J. C **74**, 2806 (2014).
[47] M. Quiros, arXiv:hep-ph/9901312.
[48] J. Zinn-Justin, arXiv:hep-ph/0005272.
[49] For instance, see P. Mati, arXiv:1601.00450.
[50] For reviews with this issue, see for instance, J. Zinn-Justin, *Quantum Field Theory and Critical Phenomenon*, 3rd ed. (Clarendon Press, Oxford, 1996).
[51] R. Percacci and G. P. Vacca, Phys. Rev. D **90**, 107702 (2014).
[52] L. Fei, S. Giombi, and I. R. Klebanov, Phys. Rev. D **90**, 025018 (2014).